

GS 2000+25: The Least Luminous Black Hole X-ray Binary

JENNIFER RODRIGUEZ,¹ RYAN URQUHART,¹ RICHARD M. PLOTKIN,² TERESA PANURACH,¹ LAURA CHOMIUK,¹
JAY STRADER,¹ JAMES C.A. MILLER-JONES,³ ELENA GALLO,⁴ AND GREGORY R. SIVAKOFF⁵

¹*Center for Data Intensive and Time Domain Astronomy, Department of Physics and Astronomy, Michigan State University, East Lansing MI 48824, USA*

²*Department of Physics, University of Nevada, 1664 N. Virginia St, Reno, Nevada, 89557, USA*

³*International Centre for Radio Astronomy Research, Curtin University, GPO Box U1987, Perth, WA 6845, Australia*

⁴*Department of Astronomy, University of Michigan, 1085 S University, Ann Arbor, MI 48109, USA*

⁵*Department of Physics, CCIS 4-183, University of Alberta, Edmonton, AB T6G 2E1, Canada*

Submitted to ApJ

ABSTRACT

Little is known about the properties of the accretion flows and jets of the lowest-luminosity quiescent black holes. We report new, strictly simultaneous radio and X-ray observations of the nearby stellar-mass black hole X-ray binary GS 2000+25 in its quiescent state. In deep *Chandra* observations we detect the system at a faint X-ray luminosity of $L_X = 1.1^{+1.0}_{-0.7} \times 10^{30} (d/2 \text{ kpc})^2 \text{ erg s}^{-1}$ (1–10 keV). This is the lowest X-ray luminosity yet observed for a quiescent black hole X-ray binary, corresponding to an Eddington ratio $L_X/L_{\text{Edd}} \sim 10^{-9}$. In 15 hours of observations with the Karl G. Jansky Very Large Array, no radio continuum emission is detected to a 3σ limit of $< 2.8 \mu\text{Jy}$ at 6 GHz. Including GS 2000+25, four quiescent stellar-mass black holes with $L_X < 10^{32} \text{ erg s}^{-1}$ have deep simultaneous radio and X-ray observations and known distances. These sources all have radio to X-ray luminosity ratios generally consistent with, but slightly lower than, the low state radio/X-ray correlation for stellar-mass black holes with $L_X > 10^{32} \text{ erg s}^{-1}$. Observations of these sources tax the limits of our current X-ray and radio facilities, and new routes to black hole discovery are needed to study the lowest-luminosity black holes.

Keywords: stars: black holes — stars: individual: GS 2000+25 — X-rays: binaries

1. INTRODUCTION

The relationship between radio luminosity (L_R) and X-ray luminosity (L_X) is one of the primary observational tools used for studying the connection between inflows (accretion) and outflows (jets) in accreting stellar-mass black holes (Corbel et al. 2013). A strong correlation exists between L_R and L_X for X-ray binaries in the low/hard and quiescent states ($\lesssim 1\%$ Eddington luminosity). In these states, a typical interpretation is that X-rays are produced through inverse Comptonization processes in the inner regions of a hot accretion flow, while the radio emission is synchrotron radiation originating from a relativistic jet (Fender et al. 2004). As a population, black holes follow a correlation $L_R \propto$

$L_X^{0.61 \pm 0.03}$ with ~ 0.3 dex of intrinsic scatter (Gallo et al. 2018). However, individual systems have been observed to follow correlations with different correlation slopes (Gallo et al. 2014), some of which even change their slopes with luminosity (e.g., Coriat et al. 2011).

Most observations of black holes in the low state were made at relatively high luminosities, but in order to fully understand the L_R – L_X relation, we must also study dim sources to constrain the behavior of the correlation at low luminosities ($L_X \lesssim 10^{33} \text{ erg s}^{-1}$). Below $L_X = 10^{32} \text{ erg s}^{-1}$, there are only three dynamically confirmed black holes with simultaneous measurements of L_X and L_R and robust distance constraints (Gallo et al. 2006, 2014; Ribó et al. 2017; Dinçer et al. 2018). While other black holes in this luminosity range have previously been observed with non-simultaneous observations, the strong short- and long-term variability (factors of $\gtrsim 3$; e.g., Miller-Jones et al. 2011; Dzib et al. 2015;

Dinçer et al. 2018) in quiescence makes comparisons between the radio and X-ray unreliable. It is also clear that individual sources show scatter about the relation when observed at different times (e.g., A0620-00, Dinçer et al. 2018), and hints of different slopes of the L_R – L_X relation for different sources (e.g., XTE J1118+480; Gallo et al. 2014). Needless to say, additional simultaneous deep radio and X-ray observations are required for quiescent black holes. There are only a handful of nearby ($\lesssim 3$ kpc) black holes, and each one represents a precious opportunity to constrain the L_R – L_X relation and probe accretion–jet coupling at low luminosities.

GS 2000+25 is one such system — a black hole X-ray binary at a distance of $2.0^{+0.6}_{-0.4}$ kpc (Harlaftis et al. 1996). GS 2000+25 was discovered by the *Ginga* satellite via its 1988 X-ray outburst (Makino & GINGA Team 1988). Using *Ginga*, Tsunemi et al. (1989) monitored GS 2000+25 for several weeks as the outburst began to decay, though the source clearly remained in the soft state. Pointed observations of GS 2000+25 were conducted in 1993 and 1994 with ROSAT (Verbunt et al. 1994), though the source was not detected down to a 1–10 keV luminosity of $< 7 \times 10^{31}$ erg s $^{-1}$ (assuming a photon index of $\Gamma = 2.1$ and $N_H = 8 \times 10^{21}$ cm $^{-2}$; Narayan et al. 1997).

Subsequent optical observations were used to dynamically confirm the X-ray binary as containing a black hole of $8.4 \pm 1.3 M_\odot$, with a K dwarf secondary, orbiting at a period of ~ 8.3 hr (Casares et al. 1995; Filippenko et al. 1995; Ioannou et al. 2004).

The first quiescent detection of GS 2000+25 in X-rays was made with *Chandra* Cycle 1 observations (Garcia et al. 2001). These data showed a significant but faint detection of the source with just five counts, yielding an X-ray luminosity of a few $\times 10^{30}$ erg s $^{-1}$. Non-simultaneous 8.46 GHz radio continuum observations from 2009 using the pre-upgrade Very Large Array using CnB and C configurations did not detect the binary in quiescence, reaching a 3σ rms sensitivity of 30.7 μ Jy (Miller-Jones et al. 2011). These observations correspond to an upper limit on the radio spectral luminosity, $< 4.4 \times 10^{17}$ erg s $^{-1}$ Hz $^{-1}$.

This study presents the first strictly simultaneous radio and X-ray observations of GS 2000+25, using the Karl G. Jansky Very Large Array (VLA) and *Chandra* X-ray Observatory, allowing us to accurately compare the system to the L_R – L_X relation. In §2, we analyze the 2016 radio and X-ray data, and revisit the archival *Chandra* data published by Garcia et al. (2001). In §3, we discuss the implications of these observations, before briefly concluding in §4.

2. DATA ANALYSIS

2.1. Radio Observations

GS 2000+25 was observed for 15 hr with the VLA on two successive days: 2016 Dec 31 and 2017 Jan 1. These two observations were each 7.5 hr long, and the 2016 Dec 31 block was entirely encompassed within our new *Chandra* observations (see §2.2.1). The VLA data were taken with C band receivers using 3-bit samplers, covering the 4–8 GHz frequency range with two 2048-MHz-wide subbands centered at 5 GHz and 7 GHz. The VLA was in its most extended A configuration, with a maximum baseline of 36.4 km. For both blocks, 3C48 was used as the bandpass and absolute flux density calibrator; it was observed at the end of each observation for 7 minutes on source. The complex gain calibrator was J2003+3034, which was observed for 1 minute between each on-source 10-minute block.

The data were processed using the Common Astronomy Software Application (CASA; McMullin et al. 2007) v5.4.0, using calibrated products provided from the VLA CASA calibration pipeline. We concatenated the two days of data together and imaged them with CASA’s `clean` task. We carried out multi-frequency synthesis imaging with frequency-dependent deconvolution (`nterms`=2) and used Briggs weighting with a robust value of 1. The resulting image, with a central frequency of 6 GHz, has a restored synthesized beam of $0.37'' \times 0.34''$ and a central rms value of 0.86μ Jy beam $^{-1}$.

No significant radio continuum source is detected at the known optical location (RA= $20^h02^m49.580^s$, Dec= $25^\circ14'11.30''$, J2000; Liu et al. 2007) of GS 2000+25. We set a 3σ upper limit of $< 2.6 \mu$ Jy on the flux density of a point source at this location (see Figure 1, top). Assuming a flat spectrum, this corresponds to a 3σ radio luminosity upper limit of $< 6.2 \times 10^{25} (d/2 \text{ kpc})^2$ erg s $^{-1}$ at a reference frequency of 5 GHz.

2.2. X-ray Observations

2.2.1. 2016 Data

Chandra observed GS 2000+25 for 55.1 ks on 2016 Dec 31, starting at UT 12:05:50 (ObsID 17861) — simultaneous with our first VLA observation for 27 ks. The target was placed at the nominal aimpoint on the S3 chip of the Advanced CCD Imaging Spectrometer (ACIS; Garmire et al. 2003).

Data were reduced following standard techniques in the *Chandra* Interactive Analysis of Observations (CIAO; Fruscione et al. 2006) software v4.8 and CALDB 4.7.0. We first reprocessed the data using `chandra_repro`, and then checked that there were no time periods with anomalously high background. Images were filtered

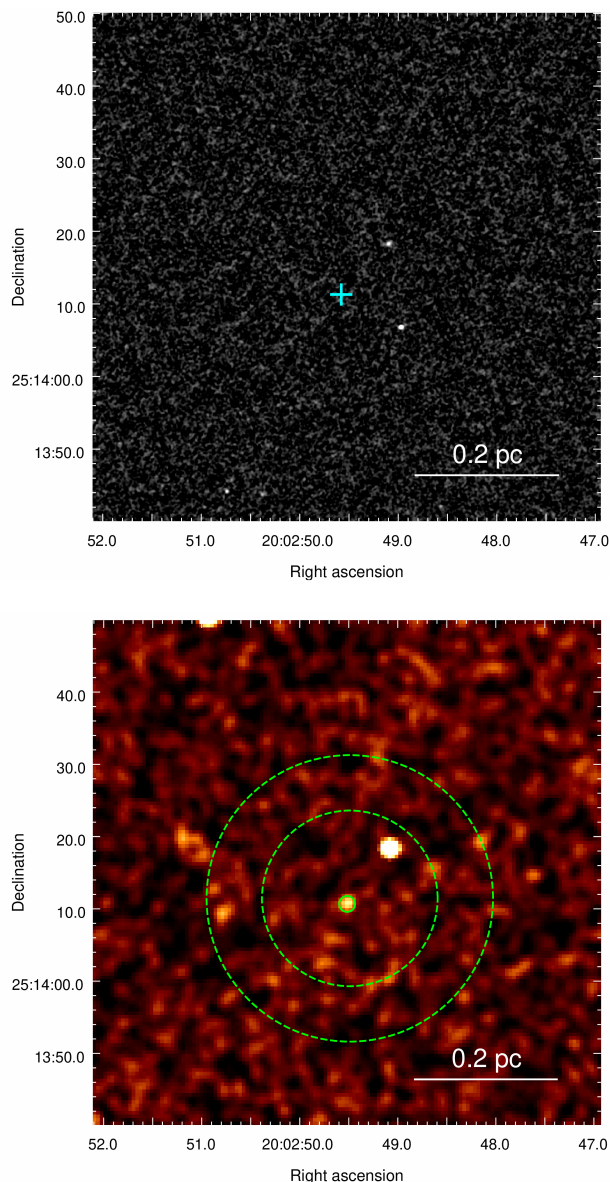


Figure 1. Top panel: VLA 6 GHz image of GS 2000+25. The optical position is marked with the cyan cross. The source is not detected, with a 3σ upper limit of $< 2.8 \mu\text{Jy}$. Bottom panel: Stacked (1999 & 2016) *Chandra* ACIS image of GS 2000+25. For visualization purposes, the image has been adaptively smoothed using a Gaussian kernel of $\sigma = 3$ pixel, with a pixel size of $0.492''$. There is a clear detection of an X-ray source associated with the binary. The source extraction region is outlined by the solid green circle, while the dashed annulus outlines the background extraction region.

from 0.5–7.0 keV to avoid energy ranges with higher background.

Source counts were extracted over a circular aperture (centered on the known optical position of GS 2000+25) with radius $1.1''$, which corresponds to the 0.9 enclosed

energy fraction (at 2.3 keV) at the position of the target’s location on the ACIS chip. Background counts were measured over a source-free annulus with inner and outer radii of $12''$ and $20''$, respectively. Within the source aperture we find 8 counts, of which 0.4 are expected to be from the background. Using the method of Kraft et al. (1991), this is a detection at the $>99\%$ level (see Figure 1, bottom). After dividing the net counts by 0.9 (as an aperture correction) and considering the 90% confidence interval from Kraft et al. (1991), we find a net count rate of $1.5^{+1.1}_{-0.8} \times 10^{-4} \text{ ct s}^{-1}$ for 0.5–7.0 keV.

Since there are too few counts for a spectral analysis, we estimate fluxes using WebPIMMS¹ and the appropriate *Chandra* Cycle 17 effective area curves. For a column density $N_{\text{H}} = 8 \times 10^{21} \text{ cm}^{-2}$ (Narayan et al. 1997) and power-law spectrum with photon index $\Gamma = 2.1$ (typical of quiescent black hole X-ray binaries; Plotkin et al. 2013; Reynolds et al. 2014), we find absorbed and unabsorbed 1–10 keV X-ray fluxes of 1.8×10^{-15} and $2.4 \times 10^{-15} \text{ erg s}^{-1} \text{ cm}^{-2}$, respectively. This equates to an unabsorbed luminosity of $1.1^{+1.0}_{-0.7} \times 10^{30} (d/2 \text{ kpc})^2 \text{ erg s}^{-1}$.

2.2.2. 1999 Archival Data

To ensure the most accurate comparison to our new observations, we re-analyzed the published quiescent X-ray observations from Garcia et al. (2001). These were obtained on 1999 Nov 5 with *Chandra*/ACIS-I and covered about 18 ks of good time (ObsID 96). Using the same analysis procedures as above, we find 5 net counts. Using $N_{\text{H}} = 8 \times 10^{21} \text{ cm}^{-2}$ and $\Gamma = 2.1$, the unabsorbed luminosity in the 1999 observation is $2.0^{+2.0}_{-1.2} \times 10^{30} (d/2 \text{ kpc})^2 \text{ erg s}^{-1}$ over the 1–10 keV band².

2.3. Distance constraints

A challenge in precisely placing low-mass X-ray binaries on the radio/X-ray correlation is that their distances are often uncertain. Here we briefly evaluate distance estimates for GS 2000+25.

So far in this work, we have used the distance of Harlaftis et al. (1996), $d = 2.0^{+0.6}_{-0.4} \text{ kpc}$. This measurement comes from a combination of measurements of the GS 2000+25 secondary: its *K* band apparent magnitude, effective temperature, and projected size (as determined by Roche geometry). The uncertainty is principally determined by the poorly-constrained inclination

¹ <http://cxc.harvard.edu/toolkit/pimms.jsp>

² Garcia et al. (2001) report luminosities over a different energy range. Converting their reported count rate to an unabsorbed 1–10 keV luminosity adopting our model parameters, our results are consistent within the uncertainties.

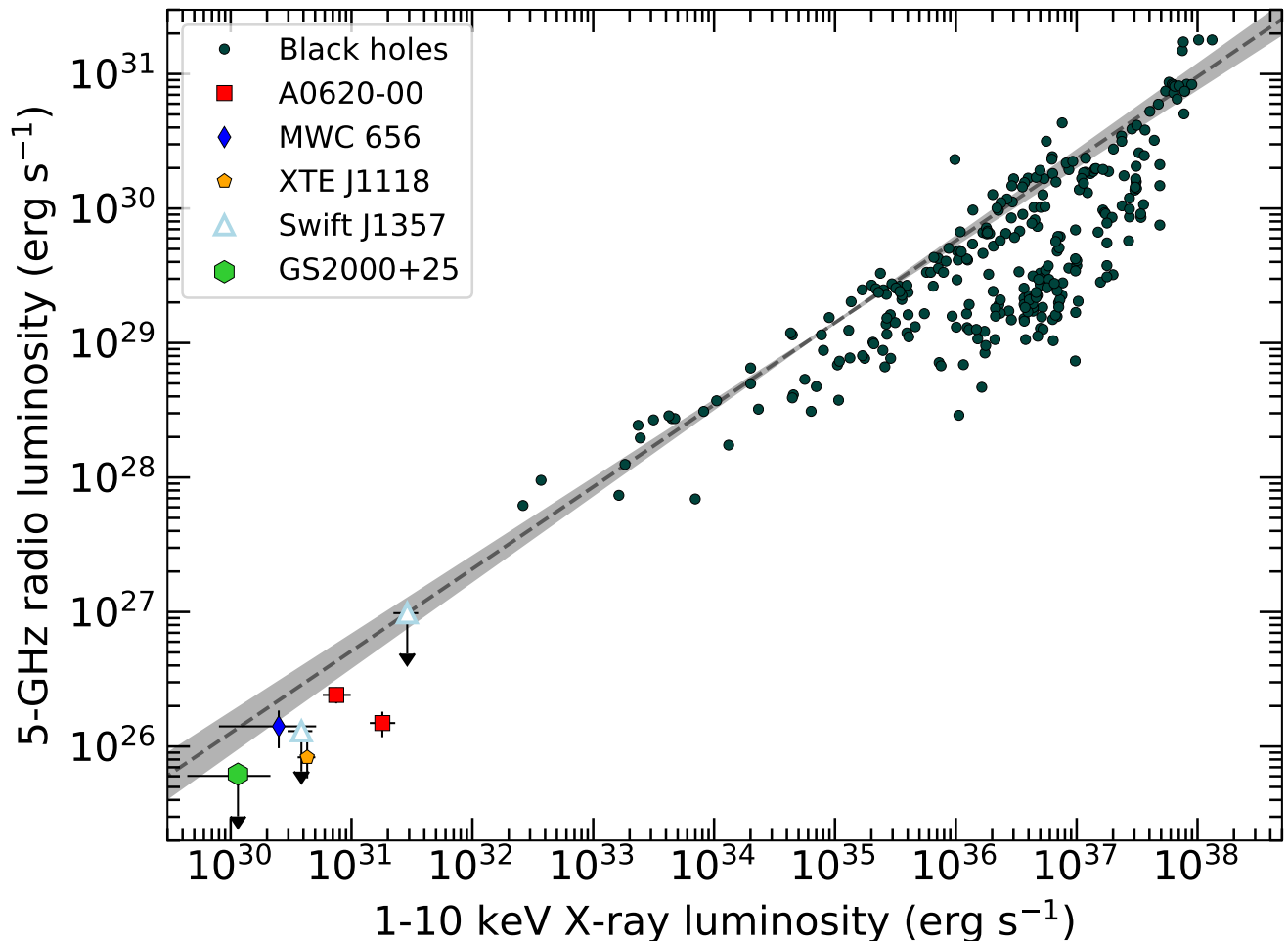


Figure 2. Radio/X-ray correlation for stellar-mass black holes, with GS 2000+25 depicted as a green hexagon. Black circles indicate hard-state black holes (Tetarenko et al. 2016a), while sources in quiescence are individually highlighted: red squares for A0620-00 (Gallo et al. 2006; Dincer et al. 2018), blue diamond for MWC 656 (Ribó et al. 2017), and orange pentagon for XTE J1118+480 (Gallo et al. 2014). Due to the large uncertainty on the distance (2.3 – 6.3 kpc), we plot the luminosity range derived from the distance extremes for Swift J1357.2-0933 (empty cyan triangles; Plotkin et al. 2016), though the distance is likely to be $\gtrsim 6$ kpc (Charles et al. 2019). The dashed line represents the best-fit radio/X-ray relation for black holes in the low/hard state from Gallo et al. (2014), with the 1σ error expressed by the shaded region.

of the binary. Relative to distance measurements determined using the optical (V) magnitude, infrared measurements are less sensitive to line-of-sight extinction and contamination from the accretion disk.

We can obtain an independent estimate of the distance by comparing the extinction of GS 2000+25 to three-dimensional reddening maps, which are of much higher quality than those available when the main papers were being written on this source two decades ago. We use the correlation between galactic extinction and the equivalent width of the Na interstellar absorption lines, $\lambda 5890$ Å and $\lambda 5896$ Å (Poznanski et al. 2012). Using the unresolved Na doublet equivalent width for GS 2000+25 reported in Charles et al. (1991), we find an interstellar extinction of $A_V = 1.11 \pm 0.25$ mag. Comparing this

extinction to two sets of three-dimensional maps, which combine *Gaia*, Pan-STARRS, and 2MASS (Green et al. 2019) or *Gaia*, 2MASS, and WISE (Chen et al. 2019), we find distances of 0.73 ± 0.05 kpc and $1.0^{+0.6}_{-0.2}$ kpc, respectively. The small uncertainty in the Green et al. (2019) estimate arises from a dust cloud in the model at ~ 0.75 kpc, beyond which the modeled extinction rises to $A_V \gtrsim 2$ mag.

We can also use the relation between hydrogen column density (n_H) and extinction (Bahramian et al. 2015) to estimate the distance. A value of $n_H = 8 \times 10^{21} \text{ cm}^{-2}$ (Narayan et al. 1997) implies $A_V = 2.85$ mag and, hence, $d = 2.0^{+0.9}_{-0.6}$ kpc (based on the Chen et al. 2019 reddening maps; the value for the Green et al. (2019) maps is similar).

The discrepancy between these optical and X-ray extinction estimates (and corresponding distance measurements) is substantial, and indeed Charles et al. (1991) mentioned that different interstellar lines in their optical spectra of GS 2000+25 implied inconsistent values for the extinction. The original Harlaftis et al. (1996) distance assumed $E(B - V) = 1.5$ and would be slightly (around 10%) larger if a lower reddening of $E(B - V) = 0.9$ were adopted, but this source of uncertainty is small compared to that in the system inclination, and in any event would not change our conclusions.

While not conclusive, there is agreement on a distance of ~ 2 kpc from modeling the infrared photometry of the secondary and the extinction implied by the X-ray data. The optical extinction may indicate a somewhat nearer distance. In any case, a distance meaningfully in excess of 2–3 kpc seems unlikely based on the available data, and thus we are confident the X-ray and radio luminosities (or limits) that we report below for GS 2000+25 are not substantial underestimates. The source might well be bright enough that a geometric parallax could be determined in a future *Gaia* data release.

3. RESULTS AND DISCUSSION

GS 2000+25 is the lowest-luminosity black hole with high-quality, simultaneous observations at both radio and X-ray wavelengths. Our upper limit on its radio luminosity is the deepest to date, constraining the spectral luminosity to be $< 1.2 \times 10^{16} \text{ erg s}^{-1} \text{ Hz}^{-1}$ (for a distance of 2.0 kpc; Harlaftis et al. 1996). Our 2016 X-ray observations measure a 1–10 keV luminosity of $1.1^{+1.0}_{-0.7} \times 10^{30} \text{ erg s}^{-1}$, which corresponds to an X-ray Eddington ratio of $\sim 10^{-9}$. Comparing our new *Chandra* observation to the re-analyzed Cycle 1 archival data, we find marginal evidence of X-ray variability. Between 1999 and 2016, the 1–10 keV unabsorbed flux of GS 2000+25 decreased by a factor of two. However, due to the low number of counts in each observation, and hence large uncertainties, we cannot conclusively confirm the presence of any variability.

Our 2016 measurements are the only simultaneous radio and X-ray observations of GS 2000+25 in the low/hard or quiescent states. For the two months following its discovery in X-ray outburst (May–June 1988; Tsunemi et al. 1989), GS 2000+25 was monitored with radio observations (1.5–15 GHz) by Hjellming et al. (1988). During this time, it appeared as a fading synchrotron source with a radio spectrum, $S_\nu \propto \nu^{-0.5}$. However, the X-ray spectrum was in the soft state throughout this period (Efremov et al. 1989), and so these X-ray and radio observations are not appropriate for placement on the $L_R - L_X$ plane.

We place GS 2000+25 on the $L_R - L_X$ plane in Figure 2, and compare it with other stellar-mass black holes in the low/hard and quiescent states. Radio luminosities for all black holes are normalized to 5 GHz assuming a flat spectrum ($S_\nu \propto \nu^0$). The black dashed line represents:

$$L_R = 4.4 \times 10^7 L_X^{0.61} \text{ erg s}^{-1} \quad (1)$$

as fit by Gallo et al. (2014) to 24 black hole X-ray binaries (essentially all of which have $L_X > 10^{33} \text{ erg s}^{-1}$).

GS 2000+25 is the fourth member of a growing population of low-luminosity quiescent black holes that constrain the $L_R - L_X$ relation at low luminosities ($L_X < 10^{32} \text{ erg s}^{-1}$), joining XTE J1118+480 (Gallo et al. 2014), MWC 656 (Ribó et al. 2017), and A0620–00 (Gallo et al. 2006; Dinger et al. 2018) at this low-luminosity extreme. A fifth source, Swift J1357.2–0933, also has strictly simultaneous and deep radio and X-ray observations in quiescence (Plotkin et al. 2016), but we do not include it because of its very uncertain distance.

It is noteworthy that all four of these quiescent black holes are below the Gallo et al. (2014) $L_R - L_X$ relation (if only slightly; see Figure 2), which is mostly determined by the radio-luminous branch of black hole X-ray binaries with $L_X > 10^{32} \text{ erg s}^{-1}$. Since the number of sources in this region is still small, one interpretation of Figure 2 is that, due to intrinsic dispersion or distance uncertainties, these quiescent sources happen to sit below the mean relation by chance (since $L_R - L_X$ is nonlinear, distance uncertainty vectors are not parallel to the relation; see e.g., Miller-Jones et al. 2011). Beyond the realm of random uncertainties, it is plausible that black hole binaries could vary in the normalization or slope of their individual $L_R - L_X$ relations. As an example, Gallo et al. (2014) argue that XTE J1118+480 shows a marginally steeper $L_R - L_X$ relation compared to the full sample of black holes.

Another possibility is that there is a true change in the nature of the $L_R - L_X$ relation at $L_X \lesssim 10^{-7} L_{\text{edd}}$. If such a change is present, it is much less extreme than implied by some scenarios, such as a transition in X-ray emission from accretion flow-dominated to jet-dominated (and an associated strong steepening of the $L_R - L_X$ relation; e.g., Yuan & Cui 2005, who suggest $L_R \sim L_X^{1.23}$). Instead, a slightly steeper exponent (compared to $L_R \sim L_X^{0.61}$ in Figure 2) might better fit the quiescent stellar-mass black holes in the low-Eddington regime. The evidence for a slope change is weak with the current observational constraints, and substantially more data would be necessary to investigate this possibility.

4. CONCLUSIONS AND FUTURE WORK

Using deep, simultaneous radio and X-ray observations, we have placed GS 2000+25 on the L_R - L_X plane. GS 2000+25 was not detected using the VLA, placing a 3σ upper limit of $< 6.2 \times 10^{25} (d/2 \text{ kpc})^2 \text{ erg s}^{-1}$ on the C-band radio luminosity. We detected GS 2000+25 with *Chandra* at an unabsorbed X-ray luminosity of $1.1^{+1.0}_{-0.7} \times 10^{30} (d/2 \text{ kpc})^2 \text{ erg s}^{-1}$. Therefore, GS 2000+25 is the least luminous black hole X-ray binary known (Gallo et al. 2008).

A number of recent papers have made significant efforts to fit the broadband spectral energy distributions of quiescent black holes, in an attempt to distinguish the different sources of emission in the system, including the donor, accretion flow, and jet (e.g., Plotkin et al. 2015; Dinger et al. 2018). Such studies have great difficulty in distinguishing among emission models owing to, among other factors, the faintness of the sources in X-ray and radio bands. Short of waiting for the next generation of observational facilities, it is critical to find new black hole X-ray binaries systems to study. Since new black hole outbursts are discovered rarely, and even fewer of these systems are nearby, there is a crucial need for surveys that can discover such systems in quiescence. Black holes can be detected and differentiated from other source classes using their L_R and L_X (e.g., Chomiuk et al. 2013; Tetarenko et al. 2016b). Combining new radio surveys (such as the VLA Sky Survey and EMU survey with ASKAP; Norris et al. 2011; Lacy et al. 2019) with new X-ray surveys (e.g., eROSITA;

Merloni et al. 2012) is a promising way forward over the next decade. Such joint radio/X-ray campaigns will compliment ongoing efforts to detect quiescent black hole binaries, like narrow-band emission line imaging (Casares 2018) and X-ray surveys (Jonker et al. 2014).

We thank an anonymous referee for helpful comments that substantially improved the paper. Support for this work was provided by the National Aeronautics and Space Administration through Chandra Award Numbers GO6-17045X, G06-17040X, GO7-18032A, and GO8-19122X issued by the Chandra X-ray Center, which is operated by the Smithsonian Astrophysical Observatory for and on behalf of the National Aeronautics Space Administration under contract NAS8-03060. JS acknowledges support from a Packard fellowship. JCAM-J is the recipient of an Australian Research Council Future Fellowship (FT140101082), funded by the Australian government. GRS acknowledges support from an NSERC Discovery Grant (RGPIN-06569-2016).

The scientific results reported in this article are based on observations made by the Chandra X-ray Observatory. The National Radio Astronomy Observatory is a facility of the National Science Foundation operated under cooperative agreement by Associated Universities, Inc. This research has made use of software provided by the Chandra X-ray Center (CXC) in the application package CIAO.

Facilities: CXO, VLA

REFERENCES

- Bahramian, A., Heinke, C. O., Degenaar, N., et al. 2015, *MNRAS*, 452, 3475
- Casares, J. 2018, *MNRAS*, 473, 5195
- Casares, J., Charles, P. A., & Marsh, T. R. 1995, *MNRAS*, 277, L45
- Charles, P., Matthews, J. H., Buckley, D. A. H., et al. 2019, *MNRAS*, 489, L47
- Charles, P. A., Kidger, M. R., Pavlenko, E. P., Prokof'eva, V. V., & Callanan, P. J. 1991, *MNRAS*, 249, 567
- Chen, B. Q., Huang, Y., Yuan, H. B., et al. 2019, *MNRAS*, 483, 4277
- Chomiuk, L., Strader, J., Maccarone, T. J., et al. 2013, *ApJ*, 777, 69
- Corbel, S., Coriat, M., Brocksopp, C., et al. 2013, *MNRAS*, 428, 2500
- Coriat, M., Corbel, S., Prat, L., et al. 2011, *MNRAS*, 414, 677
- Dinger, T., Bailyn, C. D., Miller-Jones, J. C. A., Buxton, M., & MacDonald, R. K. D. 2018, *ApJ*, 852, 4
- Dzib, S. A., Massi, M., & Jaron, F. 2015, *A&A*, 580, L6
- Efremov, V. V., Grebenev, S. A., Kaniovsky, A. S., et al. 1989, in *ESA Special Publication*, Vol. 1, Two Topics in X-Ray Astronomy, Volume 1: X Ray Binaries. Volume 2: AGN and the X Ray Background, ed. J. Hunt & B. Battrick, 15
- Fender, R. P., Belloni, T. M., & Gallo, E. 2004, *MNRAS*, 355, 1105
- Filippenko, A. V., Matheson, T., & Barth, A. J. 1995, *ApJL*, 455, L139
- Fruscione, A., McDowell, J. C., Allen, G. E., et al. 2006, in *Society of Photo-Optical Instrumentation Engineers (SPIE) Conference Series*, Vol. 6270, *Proc. SPIE*, 62701V
- Gallo, E., Degenaar, N., & van den Eijnden, J. 2018, *Monthly Notices of the Royal Astronomical Society*, 478, L132
- Gallo, E., Fender, R. P., Miller-Jones, J. C. A., et al. 2006, *MNRAS*, 370, 1351

- Gallo, E., Homan, J., Jonker, P. G., & Tomsick, J. A. 2008, *ApJL*, 683, L51
- Gallo, E., Miller-Jones, J. C. A., Russell, D. M., et al. 2014, *MNRAS*, 445, 290
- Garcia, M. R., McClintock, J. E., Narayan, R., et al. 2001, *ApJL*, 553, L47
- Garmire, G. P., Bautz, M. W., Ford, P. G., Nousek, J. A., & Ricker, George R., J. 2003, in *Society of Photo-Optical Instrumentation Engineers (SPIE) Conference Series*, Vol. 4851, *Proc. SPIE*, ed. J. E. Truemper & H. D. Tananbaum, 28–44
- Green, G. M., Schlafly, E. F., Zucker, C., Speagle, J. S., & Finkbeiner, D. P. 2019, *arXiv e-prints*, [arXiv:1905.02734](https://arxiv.org/abs/1905.02734)
- Harlaftis, E. T., Horne, K., & Filippenko, A. V. 1996, *PASP*, 108, 762
- Hjellming, R. M., Calovini, T. A., Han, X. H., & Cordova, F. A. 1988, *ApJL*, 335, L75
- Ioannou, Z., Robinson, E. L., Welsh, W. F., & Haswell, C. A. 2004, *AJ*, 127, 481
- Jonker, P. G., Torres, M. A. P., Hynes, R. I., et al. 2014, *ApJS*, 210, 18
- Kraft, R. P., Burrows, D. N., & Nousek, J. A. 1991, *ApJ*, 374, 344
- Lacy, M., Baum, S. A., Chandler, C. J., et al. 2019, *arXiv e-prints*, [arXiv:1907.01981](https://arxiv.org/abs/1907.01981)
- Liu, Q. Z., van Paradijs, J., & van den Heuvel, E. P. J. 2007, *A&A*, 469, 807
- Makino, F., & GINGA Team. 1988, *IAUC*, 4587, 1
- McMullin, J. P., Waters, B., Schiebel, D., Young, W., & Golap, K. 2007, in *Astronomical Society of the Pacific Conference Series*, Vol. 376, *Astronomical Data Analysis Software and Systems XVI*, ed. R. A. Shaw, F. Hill, & D. J. Bell, 127
- Merloni, A., Predehl, P., Becker, W., et al. 2012, *arXiv e-prints*, [arXiv:1209.3114](https://arxiv.org/abs/1209.3114)
- Miller-Jones, J. C. A., Jonker, P. G., Maccarone, T. J., Nelemans, G., & Calvelo, D. E. 2011, *ApJL*, 739, L18
- Narayan, R., Garcia, M. R., & McClintock, J. E. 1997, *ApJL*, 478, L79
- Norris, R. P., Hopkins, A. M., Afonso, J., et al. 2011, *PASA*, 28, 215
- Plotkin, R. M., Gallo, E., & Jonker, P. G. 2013, *ApJ*, 773, 59
- Plotkin, R. M., Gallo, E., Markoff, S., et al. 2015, *MNRAS*, 446, 4098
- Plotkin, R. M., Gallo, E., Jonker, P. G., et al. 2016, *MNRAS*, 456, 2707
- Poznanski, D., Prochaska, J. X., & Bloom, J. S. 2012, *MNRAS*, 426, 1465
- Reynolds, M. T., Reis, R. C., Miller, J. M., Cackett, E. M., & Degenaar, N. 2014, *MNRAS*, 441, 3656
- Ribó, M., Munar-Adrover, P., Paredes, J. M., et al. 2017, *ApJL*, 835, L33
- Tetarenko, B. E., Sivakoff, G. R., Heinke, C. O., & Gladstone, J. C. 2016a, *ApJS*, 222, 15
- Tetarenko, B. E., Bahramian, A., Arnason, R. M., et al. 2016b, *ApJ*, 825, 10
- Tsunemi, H., Kitamoto, S., Okamura, S., & Roussel-Dupre, D. 1989, *ApJL*, 337, L81
- Verbunt, F., Belloni, T., Johnston, H. M., van der Klis, M., & Lewin, W. H. G. 1994, *A&A*, 285, 903
- Yuan, F., & Cui, W. 2005, *ApJ*, 629, 408